

U-Load Dextramer®

Build multimers with your choice of peptide and peptide-receptive MHC I and MHC II alleles.



Inhibiting Oxidative Phosphorylation In Vivo Restrains Th17 Effector Responses and Ameliorates Murine Colitis

This information is current as of February 26, 2022.

Luigi Franchi, Ivan Monteleone, Ling-Yang Hao, Mark A. Spahr, Wenpu Zhao, Xikui Liu, Kellie Demock, Aditi Kulkarni, Chuck A. Lesch, Brian Sanchez, Laura Carter, Irene Marafini, Xiao Hu, Oksana Mashadova, Min Yuan, John M. Asara, Harinder Singh, Costas A. Lyssiotis, Giovanni Monteleone, Anthony W. Opipari and Gary D. Glick

J Immunol 2017; 198:2735-2746; Prepublished online 27 February 2017;

doi: 10.4049/jimmunol.1600810

<http://www.jimmunol.org/content/198/7/2735>

Supplementary Material <http://www.jimmunol.org/content/suppl/2017/02/24/jimmunol.1600810.DCSupplemental>

References This article **cites 68 articles**, 12 of which you can access for free at: <http://www.jimmunol.org/content/198/7/2735.full#ref-list-1>

Why *The JI*? [Submit online.](#)

- **Rapid Reviews! 30 days*** from submission to initial decision
- **No Triage!** Every submission reviewed by practicing scientists
- **Fast Publication!** 4 weeks from acceptance to publication

**average*

Subscription Information about subscribing to *The Journal of Immunology* is online at: <http://jimmunol.org/subscription>

Permissions Submit copyright permission requests at: <http://www.aai.org/About/Publications/JI/copyright.html>

Email Alerts Receive free email-alerts when new articles cite this article. Sign up at: <http://jimmunol.org/alerts>



Inhibiting Oxidative Phosphorylation In Vivo Restrains Th17 Effector Responses and Ameliorates Murine Colitis

Luigi Franchi,* Ivan Monteleone,[†] Ling-Yang Hao,[‡] Mark A. Spahr,[‡] Wenpu Zhao,* Xikui Liu,[‡] Kellie Demock,[‡] Aditi Kulkarni,[‡] Chuck A. Lesch,[‡] Brian Sanchez,[‡] Laura Carter,[‡] Irene Marafini,[†] Xiao Hu,[‡] Oksana Mashadova,[§] Min Yuan,[¶] John M. Asara,^{||} Harinder Singh,[#] Costas A. Lyssiotis,^{**,††} Giovanni Monteleone,[†] Anthony W. Opipari,^{‡‡} and Gary D. Glick^{§§}

Integration of signaling and metabolic pathways enables and sustains lymphocyte function. Whereas metabolic changes occurring during T cell activation are well characterized, the metabolic demands of differentiated T lymphocytes are largely unexplored. In this study, we defined the bioenergetics of Th17 effector cells generated in vivo. These cells depend on oxidative phosphorylation (OXPHOS) for energy and cytokine production. Mechanistically, the essential role of OXPHOS in Th17 cells results from their limited capacity to increase glycolysis in response to metabolic stresses. This metabolic program is observed in mouse and human Th17 cells, including those isolated from Crohn disease patients, and it is linked to disease, as inhibiting OXPHOS reduces the severity of murine colitis and psoriasis. These studies highlight the importance of analyzing metabolism in effector lymphocytes within in vivo inflammatory contexts and suggest a therapeutic role for manipulating OXPHOS in Th17-driven diseases. *The Journal of Immunology*, 2017, 198: 2735–2746.

During activation and differentiation, T cells adapt their metabolism in highly coordinated ways to provide energy and substrates for growth, trafficking, and the synthesis and secretion of immunoactive molecules (1, 2). Regulating metabolic pathways has thus emerged as an attractive approach to developing new therapeutic strategies to control immune function (3, 4).

Th17 cells are CD4⁺, αβ TCR-expressing cells that secrete the proinflammatory cytokines IL-17A, IL-17F, IL-21, and GM-CSF, which makes these cells critical in host defense against infections and cancer (5, 6). In contrast, abnormally increased Th17 cell activity can result in autoimmune and inflammatory diseases (5, 7). Th17 cells can be generated in vitro from naive CD4⁺ T cells in the presence of activating stimuli and appropriate polarizing cytokines (8–10). Under these conditions, hypoxia-inducible factor-1α (HIF1α), which upregulates the expression of glycolysis genes (11), and pyruvate dehydrogenase kinase, isozyme 1 (Pdk1), which inhibits the flux of pyruvate into the tricarboxylic acid (TCA) cycle (12), promote Th17 differentiation (13–16). Consistent with these findings, mice deficient in genes that control glycolysis have impaired Th17 differentiation in vivo (13, 15–17).

In contrast to the detailed understanding of the metabolic requirements for differentiation of naive CD4⁺ T cells into Th17, the metabolic requirements of differentiated Th17 effector cells have not been defined. At least two studies suggest that the metabolism of Th17 cells after differentiation differs from the glycolytic metabolism used during differentiation (16, 18). In particular, blocking glycolysis and/or glycolysis-linked biosynthesis is ineffective at treating Th17-driven diseases once Th17 cells are present (16, 18). Hence, metabolic targeting of Th17-driven disease processes requires analysis of the metabolism and bioenergetics of differentiated Th17 cells within in vivo inflammatory contexts.

To develop a metabolically targeted approach to control Th17-mediated inflammation, we analyzed the bioenergetics of differentiated Th17 cells and their metabolic requirements for the secretion of proinflammatory cytokines and the induction of colitis. We paid particular attention to two key parameters that influence T cell metabolism and function (19, 20). First, we compared the metabolic profiles of Th17 effector cells differentiated in vitro to those differentiated in vivo, as we and others have shown that T cells activated in vitro adapt a different metabolic phenotype than cells similarly activated in vivo (21, 22). Second, we took particular note of the inflammatory environment, comparing for the first time,

*Department of Pediatrics, University of Michigan, Ann Arbor, MI 48109; [†]Department of Systems Medicine, University of Rome Tor Vergata, 00133 Rome, Italy; [‡]Lycera Corporation, Ann Arbor, MI 48109; [§]Meyer Cancer Center, Weill Cornell Medical College, New York, NY 10065; [¶]Division of Signal Transduction, Beth Israel Deaconess Medical Center, Boston, MA 02115; ^{||}Department of Medicine, Harvard Medical School, Boston, MA 02115; [#]Division of Immunobiology, Cincinnati Children's Hospital Medical Center, Cincinnati, OH 45229; ^{**}Department of Molecular and Integrative Physiology, University of Michigan, Ann Arbor, MI 48109; ^{††}Department of Internal Medicine, University of Michigan, Ann Arbor, MI 48109; ^{‡‡}Department of Obstetrics and Gynecology, University of Michigan, Ann Arbor, MI, 48109; and ^{§§}Department of Chemistry, University of Michigan, Ann Arbor, MI 48109

ORCIDs: 0000-0003-4960-9696 (O.M.); 0000-0002-2178-5017 (M.Y.); 0000-0001-9309-6141 (C.A.L.); 0000-0003-0959-3749 (G.D.G.).

Received for publication May 9, 2016. Accepted for publication January 30, 2017.

This work was supported by a Dale F. Frey Breakthrough Scientist Award from the Damon Runyon Cancer Research Foundation (Grant DFS-09-14 to C.A.L.) and by National Institutes of Health Grant AI-47450 (to G.D.G.).

The microarray data presented in this article have been submitted to the Gene Expression Omnibus database (<http://www.ncbi.nlm.nih.gov/gds>) under accession number GSE68017.

Address correspondence and reprint requests to Prof. Gary D. Glick, Department of Chemistry, University of Michigan, 930 North University Avenue, Chemistry Building, Room 2819, Ann Arbor, MI 48109. E-mail address: gglick@umich.edu

The online version of this article contains supplemental material.

Abbreviations used in this article: CD, Crohn disease; 2-DG, 2-deoxyglucose; ECAR, extracellular acidification rate; GSEA, gene set enrichment analysis; HIF1α, hypoxia-inducible factor-1α; IBD, inflammatory bowel disease; LPMC, lamina propria mononuclear cell; OCR, oxygen consumption rate; OXPHOS, oxidative phosphorylation; Pdk1, pyruvate dehydrogenase kinase, isozyme 1; PPP, pentose phosphate pathway; ROR, retinoic acid-related orphan receptor; siRNA, small interfering RNA; TCA, tricarboxylic acid; TNBS, 2,4,6-trinitrobenzenesulfonic acid; UC, ulcerative colitis.

Copyright © 2017 by The American Association of Immunologists, Inc. 0022-1767/17/\$30.00

to our knowledge, the metabolic requirements of cells isolated from normal lymphoid tissues with those from inflammatory lesions.

Materials and Methods

Mice

C57BL/6 mice were obtained from Charles River Laboratories. OT-II mice (B6.Cg-Tg (Tcr α Tcr β)425Cbn/J), SJL mice (B6.SJL-Ptpr^{ca} Pep3^b/BoyJ), and IL-17GFP knock-in mice (C57BL/6-*Il17a*^{tm1Bcgen/J}) were purchased from The Jackson Laboratory. Mice were kept under specific pathogen-free conditions and provided with food and water ad libitum. The animal studies were conducted under protocols approved by the University of Michigan Committee on Use and Care of Animals.

PBMCs and biopsy specimens

PBMCs from healthy subjects and patients with inflammatory bowel disease (IBD) were isolated via Ficoll gradient fractionation and treated overnight with indicated compounds. All experiments using human PBMCs were collected in accordance with the University of Michigan Institutional Review Board, and written informed consent was obtained.

Ileum intestinal biopsy samples were taken from two patients with Crohn disease (CD) undergoing intestinal resection due to disease severity and inadequate responses to medical treatment. Biopsy specimens were obtained from an inflamed area of the large intestine of a patient with active ulcerative colitis (UC) and were used to isolate lamina propria mononuclear cells (LPMCs). One CD patient and the UC patient were receiving corticosteroids, and the remaining CD patient was treated with mesalazine. Each patient who took part in the study gave written informed consent, and the study protocol was approved by the local Ethics Committees (Tor Vergata University Hospital, Rome, Italy).

In vitro Th17 differentiation

Naive cells were isolated from the spleens of 8- to 12-wk-old mice using a CD4⁺CD62L⁺ T cell isolation kit II (Miltenyi Biotec) or an EasySep mouse naive CD4⁺ T cell isolation kit (Stemcell Technologies) following the manufacturers' protocols. Cells (100,000–200,000) were plated in RPMI 1640 (Corning Cellgro) and supplemented with 10% heat-inactivated FBS (HyClone), 1% GlutaMAX (Life Technologies), 1% penicillin/streptomycin (Sigma-Aldrich), and 0.1% 2-ME (Life Technologies) on anti-CD3-coated (2.5 μ g/ml; BD Biosciences) 96-well plates with anti-CD28 (10 μ g/ml; BD Biosciences) and Th17 differentiation mixture (see below) for 4 d in a 37°C incubator with 5% CO₂. Alternatively, splenocytes from OT-I and OT-II mice were cultured with up to 0.5 μ g/ml OVA_{257–264} peptide for OT-I and OVA_{323–339} peptide for OT-II (RS Synthesis) and supplemented with a Th17 differentiation mixture. Unless otherwise stated, Th17 differentiation mixture was prepared with IL-1 β (10 ng/ml), IL-6 (10 ng/ml), IL-23 (10 ng/ml), and human TGF- β (2.5 ng/ml). All cytokines were purchased from R&D Systems. In vitro-differentiated Th17 cells were >90% CD45.1⁺CD4⁺ at the end of differentiation.

In vivo Th17 differentiation

Naive cells (~100,000) isolated from OT-I or OT-II mice were transferred into B6.SJL mice by tail vein injection. Six to 16 h later, mice were immunized s.c., two to four sites per mouse, with 50 μ l of a 2:1:1 mixture of *Mycobacterium tuberculosis* H37 Ra (Difco), 100 mg dissolved in 10 ml of CFA (Sigma)/OVA_{323–339} peptide (4 μ g/ml water)/PBS. Cells from lymph nodes and spleens were isolated 7–9 d postimmunization, subjected to RBC lysis (Sigma-Aldrich), filtered through a 70- μ m cell strainer (Max Scientific), and purified by surface CD4 MicroBeads (Miltenyi Biotec, 130-049-201). In experiments analyzing cytokine expression, donor cells (CD4⁺CD45.2⁺) and recipient cells (CD4⁺CD45.1⁺) were gated by FACS. When higher purity donor cells were required, CD4⁺ cells were sorted by flow cytometry using either IL-17GFP or PE-CD45.2 surface marker (1:500; eBioscience, 12-0454-82). Sorted in vivo-differentiated Th17 cells were >90% CD4⁺CD45.2⁺. Alternatively, naive cells (~100,000) isolated from OT-II (Thy1.1⁺Thy1.2⁺) mice were transferred into B6 (Thy1.1⁺Thy1.2⁺) mice by tail vein injection. After immunization as above, lymph node and splenic CD4⁺ T cells were enriched by negative selection using a Miltenyi Biotec CD4⁺ T cell isolation kit followed by positive selection with anti-CD90.1-PE (BD Biosciences) and anti-PE MicroBeads. Sorted in vivo-differentiated Th17 cells were typically >80% CD4⁺CD90.1⁺.

Lamina propria isolation

Dissected mucosa were freed of mucus and epithelial cells sequentially with DTT and EDTA, and then digested with 2 mg/ml Liberase (Roche) as previously described (23). After digestion, the medium containing the

mononuclear cells was collected and centrifuged at 400 \times g for 10 min. After two washes in calcium- and magnesium-free HBSS, the pellet was resuspended in 40% Percoll solution. Two microliters each of 100, 60, 40, and 30% Percoll were layered in a 15-ml tube. The tube was centrifuged at 400 \times g for 25 min, and LPMCs were collected from the interface at the 60–40% Percoll layers.

Cell sorting

Cells were harvested at the end of the differentiation protocol, counted, and resuspended to 5 \times 10⁶/ml of 1% FBS/PBS prior to passing through a 50- μ m filter (Partec) and sorted on a MoFlo Astrios or MoFlo XDP (Beckman Coulter) at the University of Michigan Flow Cytometry Core. After sorting, cells were washed once with full media and stored as pellet at –80°C for RNA or protein extraction.

Intracellular staining

Cells were processed for intracellular staining following the manufacturer's protocol (eBioscience, 88-8823-88). Mouse Abs used were anti-IL-17a (clone eBio17B7; eBioscience), anti-CD4 (clone eBioRM4-5; eBioscience), anti-IFN- γ (clone XMG1.2; eBioscience), anti-Foxp3 (clone FJK-16S; eBioscience), anti-CD62L (clone MEL-14; eBioscience), anti-CD45.2 (clone 104; eBioscience), anti-CD44 (clone IM7; eBioscience), retinoic acid-related orphan receptor (ROR) γ t (clone AFKJS-9; eBioscience), and anti-CD90.1 (clone OX-7; BD Biosciences). Murine LPMCs were stained with the following Abs: anti-CD45-allophycocyanin-Cy7 (1:50, final dilution, clone 30f11; BD Biosciences); anti-CD3-Pacific Blue (1:50, final dilution, clone 500a2; BD Biosciences); anti-CD8-FITC (1:50, final dilution; clone 53-6.7; BD Biosciences), and intracellularly with anti-IL-17A-allophycocyanin (1:50 final dilution, clone Ebio17b7; eBioscience); and anti-IFN- γ -PE-Cy7 (1:50 final dilution, clone XMG1.2; BD Biosciences). Human Abs used were anti-human CD3 from eBioscience (clone OKT3) and anti-human IL-17a Ab (clone eBio64CAP17). Human LPMCs were stained with the following Abs: anti-CD45-allophycocyanin-H7 (1:50, final dilution, clone 2D1; BD Biosciences) and anti-CD3-Pacific Blue (1:50, final dilution, clone UCHT1; BD Biosciences). To assess the intracellular expression of IFN- γ and IL-17A, cells were stained with the following Abs: anti-IFN- γ -allophycocyanin (1:50 final dilution, clone 25723.11; BD Biosciences) and anti-IL-17A-PE (1:50, final dilution, clone 033-782; BD Biosciences). Where indicated, cells were stimulated with PMA (Sigma-Aldrich), ionomycin calcium salt (Sigma-Aldrich), and brefeldin A (eBioscience) for 4–5 h prior to fixation in 2% formaldehyde/PBS (Thermo Scientific). Cells were analyzed using a FACSVerse cytometer and FACSuite software (BD Biosciences).

Anti-CD3 activation in vivo

Female C57BL/6 mice received compound at specified dose or vehicle (40% DMSO/PBS) via i.p. injection in 200 μ l. One hour later, anti-CD3e (5 μ g per mouse) (BD Biosciences) was injected i.p. in PBS. Four hours after anti-CD3e injection, serum was collected by cardiac puncture and cytokines were analyzed by ELISA.

Seahorse measurements

Cells (7 \times 10⁵) were plated per well on an XF24 plate coated with 0.5 mg/ml poly-D-lysine (Sigma-Aldrich), centrifuged in 100 μ l of extracellular flux (XF) media supplemented with 1 mM sodium pyruvate (Sigma-Aldrich), 11 mM glucose (Sigma-Aldrich), and 1% FBS (pH 7.4), then filtered through a 0.22- μ m filter. Extracellular flux (XF) media (530 μ l) was then added to each well and incubated for 30 min in a CO₂-free incubator at 37°C, then run per the manufacturer's protocol with oligomycin, carbonyl cyanide 4-(trifluoromethoxy)phenylhydrazone, and antimycin A injections in ports A, B, and C, respectively.

Cell proliferation analysis

Naive cells were labeled with 10 μ M CFSE (Life Technologies) in 1 ml of RPMI 1640 plus 2% FBS for 10 min at 37°C, then washed with RPMI 1640 and resuspended into full medium culture. For in vivo measurements, 2 \times 10⁶ labeled cells were transferred through tail vein injection into B6.SJL mice.

Lactate measurement

Sorted in vivo Th17 cells and in vitro Th17 cells were plated at 100,000 cells per well in a 96-well plate and treated with indicated compounds. After the indicated time, cells were pelleted and supernatants from triplicate cultures were analyzed by the colorimetric method using a glycolysis cell-based assay kit (Cayman Chemical) according to the manufacturer's protocol.

ATP measurement

Sorted *in vivo* Th17 cells and *in vitro* Th17 cells were plated at 100,000 cells per well in a 96-well plate and treated with the indicated compounds. After the indicated time, cells were pelleted and lysed with a lysis buffer from an ATP bioluminescence assay kit CLS II (Roche Applied Science) supplemented with Halt protease inhibitor cocktail (Thermo Scientific) and Halt phosphatase inhibitor cocktail (Thermo Scientific) prior to heat extraction. To determine the intracellular ATP level, the lysate was processed according to the manufacturer's protocol. Analysis was performed in triplicate cultures.

Real-time PCR

RNA was isolated with RNeasy (Qiagen) according to the manufacturer's instructions. RNA was reverse transcribed using a high-capacity cDNA reverse transcription kit (Applied Biosystems), and cDNA was then used for quantitative PCR by a SYBR Green gene expression assay on an ABI 7900HT analyzer (Applied Biosystems). Primer sequences are as follows: *hif1a* forward, 5'-CGGCGAGAACGAGAAGAA-3', reverse, 5'-AAACTT-CAGACTCTTGTCTCG-3'; *pdh1* forward, 5'-GGACTTCGGGTCAAGTGAATGC-3', reverse, 5'-TCCTGAGAAGATTGTCGGGGA-3'; *rorc2* forward, 5'-CCACAGATCTGCAAGGGATC-3', reverse, 5'-CCGCTGAGAGGGC-TTCAC-3'; *foxp3* forward, 5'-TGGCAGAGAGGTATTGAGGG-3', reverse, 5'-CTCGTCTGAAGGCAGAGTCA-3'; *Ldha* forward, 5'-CTGGGTCTG-GGAGAACAT-3', reverse, 5'-GTGCCAGTTCTGGGTAAAG-3'; *aldoa* forward, 5'-TCAGTGTCTGGGTATGGGTG-3', reverse, 5'-GCTCCTTAGT-CCTTTCGCCT-3'; *hk2* forward, 5'-TGATCGCCTGCTTATTCACGG-3', reverse, 5'-AACCGCTAGAAATCTCCAGA-3'; *β-actin* forward, 5'-ATG-GAGGGGAATACAGCCC-3', reverse, 5'-TTCTTTGCAGCTCCTTCGTT-3'.

For hypoxia pathway activity, an RT² Profiler mouse hypoxia signaling pathway PCR array (Qiagen) was used following the manufacturer's protocol.

Gene expression profiling

Microarray analysis was performed on sorted CD4⁺IL-17GFP⁺ cells isolated from *in vitro* or *in vivo*-differentiated Th17. RNA was extracted with an RNeasy Plus mini kit (Qiagen) and samples were processed and analyzed at the University of Michigan Microarray Core Facility with a GeneChip mouse gene 1.0 ST array (Affymetrix). RNA was analyzed on an Agilent 2100 bioanalyzer (Agilent Technologies). All samples had a >9 RNA integrity number. Microarray quality control was performed with R (Bioconductor). The data were processed with robust multichip average normalization. Technical replicates were averaged for fold change. Genes were considered differentially expressed when they were >log₂-fold different. The microarray data are available in the Gene Expression Omnibus database (<http://www.ncbi.nlm.nih.gov/gds>) under accession number GSE68017.

Gene set enrichment analysis

All of the genes differentially expressed by >log₂-fold difference between *in vivo* (CD45.2⁺CD4⁺) or *in vitro* (CD4⁺)-differentiated Th17 cells were selected and analyzed using gene set enrichment analysis (GSEA). Three GSEA tests were employed using default program settings, testing the complete 2 log-fold gene set.

Transfection of small interfering RNA

Splenocytes from OT-II mice were cultured with up to 0.5 μg/ml OVA_{323–339} peptide (RS Synthesis) and supplemented with a Th17 differentiation mixture as described above. After 3–4 d, cells were nucleofected with 4D-Nucleofector according to the Amaxa protocol (Lonza). Briefly, 5 × 10⁶ cells were resuspended in 98 μl of nucleofector solution V4XP with 300 pM ON-TARGETplus small interfering RNA (siRNA) SMARTpool (GE Healthcare Dharmacon), transferred to a cuvette, and then electroporated using the DN-100 pulsing parameter. Cells were immediately transferred into wells containing a 37°C prewarmed culture medium and used 1 d after electroporation.

Animal disease models

For induction of acute colitis, 2.5 mg of 2,4,6-trinitrobenzenesulfonic acid (TNBS) in 50% ethanol was administered to lightly anesthetized mice through a 3.5 French catheter inserted into the rectum on day 0. The catheter tip was inserted 4 cm proximal to the anal verge, and 150 μl of fluid was slowly instilled into the colon, after which the mouse was held in a vertical position for 30 s. Starting at day 1 mice received an i.p. dose of vehicle (0.01% DMSO in PBS) or oligomycin (0.25 mg/kg) once a day, or ursolic acid orally (0.75 mg/kg in 1% gum acacia) twice a day. On day 2, colon tissue was collected for histology. Alternatively, colitis was induced by

giving mice water containing 3% dextran sodium sulfate (molecular weight of 36,000–50,000; MP Biomedicals) for 3 d.

For the induction of psoriasis, Aldara (a 5% cream of imiquimod; 3M Pharmaceuticals) was applied to the ear of mice daily for 5 d. Starting at day 1 mice received an i.p. dose of vehicle (0.01% DMSO in PBS) or oligomycin (0.25 mg/kg) once a day, or ursolic acid orally (0.75 mg/kg in 1% gum acacia) twice a day.

Histology

From the colitis animal models, upon necropsy, colon tissue was separated and Swiss rolls were prepared. Tissues were fixed in 10% buffered formalin and paraffin embedded. The sections (5 μm) were stained with H&E. A pathology score (0–10) was determined based on analysis of the following: goblet cell hyperplasia, crypt lymphocytic infiltrate, surface mucosa ulceration, mucosa prolymphocytic infiltrate, lamina propria fibrosis, lamina propria crypt abscess, crypt dilatation, crypt hyperplasia, and crypt branching. An experienced veterinary pathologist without knowledge of the tissues' origin performed histologic scoring.

Measurements of cytokines

Cytokines were measured in cell-free culture supernatants of triplicate cultures by ELISA kits (R&D Systems) at the University of Michigan Cancer Center Immunology Core.

Metabolomics

Naive (CD4⁺) cells from nonimmunized OT-II mice, *in vivo* Th17 (CD4⁺CD90.1⁺) cells, and *in vitro* Th17 (CD4⁺CD90.1⁺) cells were purified by magnetic sorting. Immediately after isolation, cells were cultured in RPMI 1640 in the presence of an equimolar concentration of unlabeled and isotope-labeled D-glucose-¹³C₆ (Sigma-Aldrich, catalog no. 660663) or L-glutamine-¹³C₅ (Sigma-Aldrich, catalog no. 605166). After 3 h, T cell pellets were extracted in 80% methanol at dry ice temperatures, and metabolite fractions corresponding to input cell numbers were dried using a SpeedVac in preparation for liquid chromatography–tandem mass spectrometry. Metabolomics analyses were performed and the data were processed and analyzed as described in the literature (24, 25).

Statistical analysis

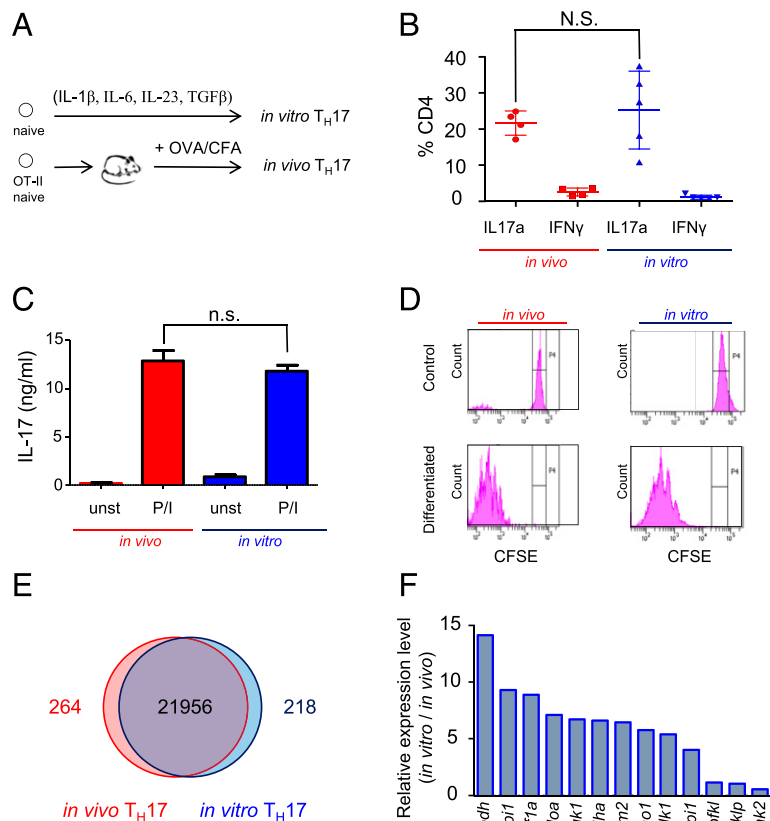
Statistical analysis was conducted using a two-tailed unpaired or paired Student *t* test using Prism (GraphPad Software). A *p* value ≤ 0.05 was considered significant. Results were considered reproducible when all independent experiments had comparable *p* values that were significant.

Results

To determine whether Th17 cells differentiated *in vivo* depend on the same metabolic processes as those previously described for cells differentiated *in vitro* (14, 17, 26), protocols were optimized to produce populations of Th17 cells *in vivo* and *in vitro* that had nearly equivalent expression of IL-17 and RORγt with limited levels of IFN-γ and Foxp3 (Supplemental Fig. 1). To generate cells *in vivo*, OT-II spleen cells were transferred to syngeneic wild-type host animals and then activated by immunization with OVA peptide in CFA (Fig. 1A). *In vitro*-differentiated Th17 cells were generated by placing naive T cells in culture and activating them with agonistic anti-CD3 and anti-CD28 Abs or by activating OT-II T cells with OVA-pulsed APCs in the presence of IL-1β, IL-6, IL-23, and TGF-β (Fig. 1A).

The proportion of CD4⁺ cells with detectable intracellular IL-17 was maximal after differentiation for 4 d *in vitro* and for 7 d *in vivo* (Supplemental Fig. 1). Notably, the *in vivo*-differentiated CD4⁺ T cells, generated after transfer of 10⁵ donor cells, expressed IL-17, RORγt, but not IFN-γ or Foxp3 (Fig. 1B, Supplemental Fig. 1C, 1D), at levels that were comparable to those of T cells generated *in vitro* with IL-1β, IL-6, IL-23, and TGF-β. Importantly, they secreted equivalent amounts of IL-17 in response to stimulation with PMA and ionomycin (Fig. 1C). Analysis by CFSE labeling showed that a similar number of cell divisions was achieved in cells differentiated for 4 d *in vitro* and 7 d *in vivo* (Fig. 1D).

FIGURE 1. Differential expression of genes controlling glycolysis in in vivo- and in vitro-differentiated Th17 cells. **(A)** Systems used to generate in vitro and in vivo Th17 cells. **(B and C)** In vivo (red)- and in vitro (blue)-differentiated Th17 cells stimulated with PMA/ionomycin. The percentage of CD4⁺IL-17a⁺ and CD4⁺IFN- γ ⁺ cells was determined by FACS (B), and the production of IL-17 in cell-free supernatant from triplicate cultures was determined by ELISA (C). **(D)** Cellular replication profile of in vivo (red)- and in vitro (blue)-differentiated Th17 cells assessed using CFSE dilution and FACS in cells before (Control) and after differentiation (Differentiated). **(E)** Gene expression of in vivo-differentiated Th17 cells (CD45.2⁺CD4⁺IL-17GFP⁺) (red circle) and in vitro-differentiated Th17 cells (CD45.1⁺CD4⁺IL-17GFP⁺) (blue circle) analyzed by microarray. Common and differential expression of genes (>2 log) is shown in a Venn diagram. **(F)** Expression of glycolytic enzymes graphed as a ratio of in vitro/in vivo-differentiated Th17 cells analyzed by quantitative PCR. **(B)** Plot of four (in vivo) and five (in vitro) independent experiments. **(C), (D), and (F)** are representative of three independent experiments. Error bars represent SEM. N.S., not significant (unpaired Student *t* test).



Having optimized the differentiation conditions, we compared the gene expression profiles of in vitro- and in vivo-derived Th17 cells. To isolate purified Th17 cells, OT-II mice were crossed with syngeneic IL-17GFP knock-in mice to generate F₁ animals that expressed the IL-17GFP reporter and OVA-specific TCR. These mice were used to isolate and characterize gene expression selectively in CD4⁺IL-17GFP⁺ T cells, which represented ~2% of the T cells after in vitro or in vivo differentiation. Importantly, the purified Th17 cells were not restimulated with PMA and ionomycin prior to RNA isolation and gene expression analysis, so as to provide a more biologically informative comparison of the transcriptomes of the in vitro versus in vivo Th17-differentiated states. More than 98% of all genes were expressed equivalently in the in vitro- and in vivo-derived cells (Fig. 1E). GSEA was applied to identify predefined gene sets with statistically significant concordant differences between in vitro and in vivo conditions (Table I). Gene sets defined as ROR γ -regulated transcripts or linked to differentiated Th17 cells were, as expected, expressed equivalently in the in vitro- and in vivo-differentiated Th17 cells (Table I). Conversely, multiple metabolism-related gene sets defined by the KEGG pathway database, including glycolysis-related genes, had significantly lower concordant expression in in vivo-differentiated cells. Lower expression of glycolytic genes in in vivo-differentiated Th17 cells was confirmed using quantitative RT-PCR by measuring transcript levels of 13 selected glycolytic enzymes, all of which were lower in in vivo cells (Fig. 1F). Remarkably, both HIF1 α and Pdk1, two genes that have been previously shown to regulate Th17 differentiation via controlling glycolysis, were substantially more highly expressed in the in vitro-generated effector Th17 cells. These data suggested that in vivo-differentiated IL-17⁺ cells function with significantly reduced utilization of glycolysis.

In vivo Th17 cells exhibit low glycolysis

To determine whether glycolytic activity differed between Th17 cells differentiated in vivo and in vitro as predicted by the gene expression profiles, we measured the rate of lactate production. The in vivo-differentiated Th17 cells exhibited a 2-fold lower rate of lactate production than did the in vitro-generated counterparts (Fig. 2A). To further interrogate and compare glucose metabolism in these cell types, we analyzed the abundance of metabolites in glycolysis and the pentose phosphate pathway (PPP) using targeted mass spectrometry-based metabolomics (25). Indeed, when normalized to the levels in in vitro-differentiated cells, the in vivo-differentiated Th17 cells had dramatically smaller metabolite pool sizes across both pathways (Fig. 2C, 2D).

To exclude the possibility that the reduced glycolytic metabolism of in vivo-differentiated Th17 cells was simply due to the isolation procedure and brief ex vivo manipulation, we activated OVA-specific,

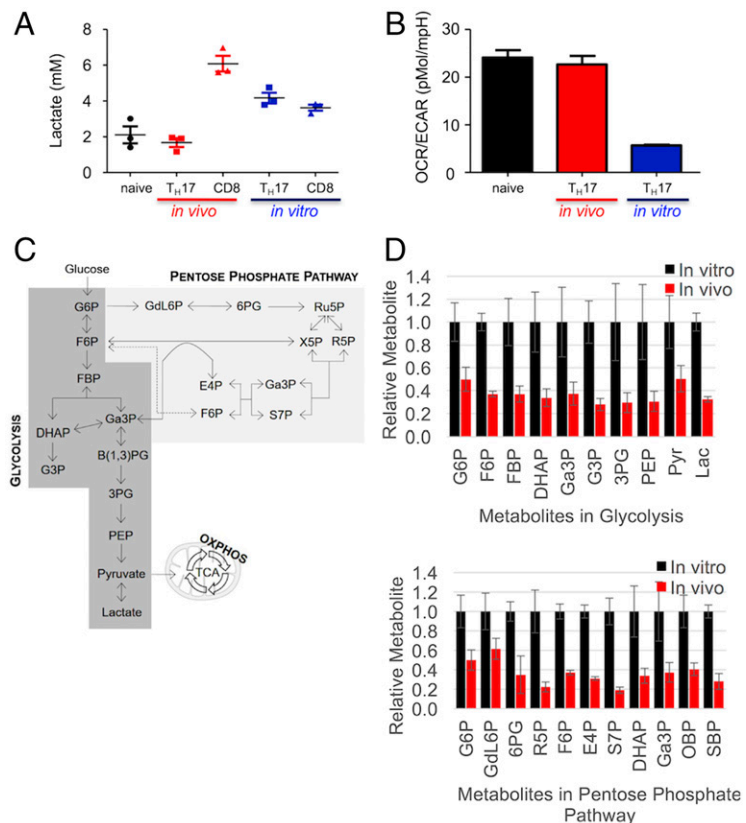
Table I. Results of GSEA

Pathway	NES	<i>p</i> Value	FDR (<i>q</i> Value)
OXPHOS	-1.79	0.0	0.006
FA Met	-1.95	0.002	0.001
Glycolysis/ gluconeogenesis	-1.64	0.004	0.02
Citrate cycle	-1.75	0.002	0.009
PPP	-1.66	0.012	0.017
Th17 signature	-1.37	0.094488	0.094
TFs associated to ROR γ	-0.73	0.883019	0.883

GSEA of the running enrichment score based on fold change of in vitro Th17 (CD45.1⁺CD4⁺IL-17GFP⁺) versus in vivo Th17 (CD45.2⁺CD4⁺IL-17GFP⁺).

FA Met, fatty acid metabolism; FDR, false discovery rate; NES, normalized enrichment score; TF, transcription factor.

FIGURE 2. In vivo-differentiated Th17 cells are oxidative. **(A)** Lactate concentration was determined in cell-free supernatant from triplicate cultures of naive CD4 cells, in vivo-differentiated Th17 cells ($CD4^+CD90.1^+$), in vivo CD8 cells ($CD8^+CD90.1^+$), in vitro Th17 cells, or in vitro CD8 cells stimulated with PMA/ionomycin. **(B)** OXPHOS and glycolysis of naive, in vivo (red)-differentiated, and in vitro (blue)-differentiated Th17 cells was analyzed via OCR and ECAR on a Seahorse bioanalyzer and expressed as OCR/ECAR ratio. **(C)** Schematic depiction of glucose metabolism in glycolysis, the PPP, and the TCA cycle. **(D)** Relative metabolite pool sizes normalized to those in the in vitro-derived Th17 cells for each of the metabolites in glycolysis (top) and the PPP (bottom). Metabolic profiles for in vitro-derived Th17 cells are depicted in black and in vivo Th17 profiles in red. Error bars represent the SEM for $n = 3$, and data are representative of four independent experiments. DHAP, dihydroxyacetone phosphate; E4P, erythrose 4-phosphate; FBP, fructose bisphosphate; F6P, fructose 6-phosphate; Ga3P, glyceraldehyde 3-phosphate; GdL6P, glucono- δ -lactone 6-phosphate; G3P, glycerol 3-phosphate; G6P, glucose 6-phosphate; Lac, lactate; OBP, octulose bisphosphate; PEP, phosphoenolpyruvate; 3PG, 3-phosphoglycerate; 6PG, 6-phosphogluconate; Pyr, pyruvate; R5P, ribose 5-phosphate; Ru5P, ribulose 5-phosphate; SBP, sedoheptulose bisphosphate. S7P, sedoheptulose 7-phosphate; X5P, xylulose 5-phosphate.



OT-I $CD8^+$ T cells in vivo by injection of OVA peptide, similarly isolated them, and measured their rate of lactate production. As seen in Fig. 2A, $CD8^+$ T cells activated in vivo demonstrated much higher rates of lactate production than did $CD4^+$ Th17 cells, thereby suggesting the metabolic program in the latter is not simply attributable as a procedure-related effect.

In vivo Th17 cells are oxidative

The balance between ATP synthesis from glycolysis and oxidative phosphorylation (OXPHOS) can be compared among different cell populations by calculating the ratio of the oxygen consumption rate (OCR) to the extracellular acidification rate (ECAR), with the latter being primarily attributed to lactic acid production from glucose through glycolysis (21, 27). Because in vivo-differentiated Th17 effectors use less glycolysis, we reasoned that their balance of OXPHOS and glycolysis might be shifted toward oxidative metabolism compared with in vitro-differentiated Th17 cells. OCR and ECAR measurements showed that in vivo-differentiated Th17 cells possess a significantly higher OCR/ECAR ratio than in vitro cells when measured immediately after isolation (Fig. 2B). This difference is primarily accounted for by reduced glycolysis in the in vivo-generated cells (Fig. 2D, Supplemental Fig. 2A) and has also been observed in T cells activated in vivo by alloantigen (21).

To exclude the possibility that differences in the OCR/ECAR ratios could be explained by the different stimuli used to activate T cells in vitro than those used in vivo, we compared OCR/ECAR values of T cells activated in vitro by anti-CD3/anti-CD28 stimulation under polarizing conditions to OT-II T cells activated by OVA-pulsed APCs. Th17 cell populations differentiated in response to either stimulation protocol in vitro had lower OCR/ECAR values compared with Th17 cells differentiated in vivo (Supplemental Fig. 2B). Additionally, stimulation of differentiated Th17 cells with PMA and ionomycin, which is commonly used to increase IL-17 production, did not affect the OCR/ECAR balance (Supplemental Fig. 2B).

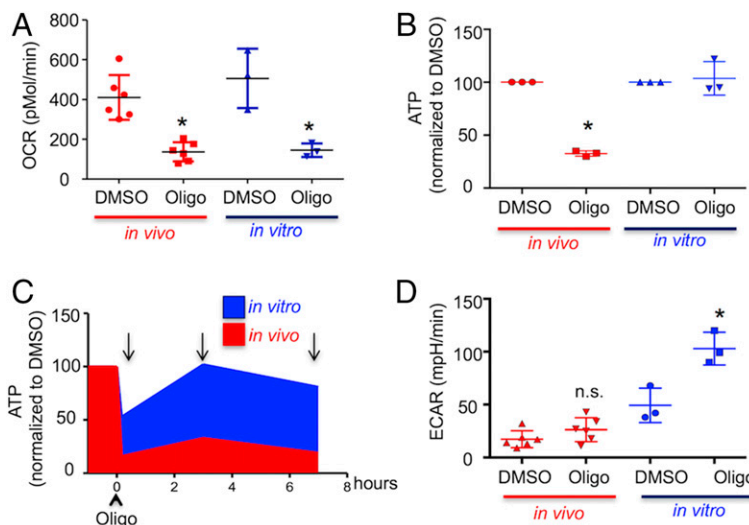
Because there is often a reciprocal relationship between levels of ATP generated by glycolysis and OXPHOS, the differences in OCR/ECAR values suggest that ATP levels in in vivo-differentiated Th17 cells should be more dependent on OXPHOS than in in vitro cells. To test this hypothesis, cells were treated for 4 h with oligomycin, a selective inhibitor of mitochondrial ATP synthase. Oligomycin reduced OCR in both the in vitro- and in vivo-differentiated Th17 effector cells to roughly comparable levels (Fig. 3A). In contrast, after 3 h, oligomycin reduced the intracellular ATP concentration by 70% in the in vivo Th17 cells, whereas ATP levels in the in vitro cells were unchanged from control (Fig. 3B). When intracellular ATP levels were assessed over the time of oligomycin treatment, there was an initial drop in ATP in both the in vitro and in vivo cells; ATP levels in the in vitro Th17 effector cells returned to baseline, whereas ATP levels remained low in the in vivo effector Th17 cells. The transient drop in ATP in the in vitro effector Th17 cells (Fig. 3C), followed by the recovery of ATP production in the presence of oligomycin, demonstrates the cells' metabolic adaptability and suggests that in vitro-differentiated cells increase glycolysis to compensate for energy stress (28).

In vitro Th17 cells activate glycolysis when OXPHOS is blocked

The ability to adapt metabolism by increasing glycolytic flux to meet energy demands in the face of oxygen deprivation is well established in many tissue types. However, some cell types lack this capacity (29), which presents a putative liability that could be exploited therapeutically. Therefore, we tested whether in vivo-generated Th17 cells lack metabolic flexibility; namely, the ability to increase glycolysis to preserve effector function when OXPHOS is blocked.

Consistent with this possibility, oligomycin doubled the ECAR in in vitro Th17 cells but had no effect on the ECAR of

FIGURE 3. In vivo Th17 cells are metabolically inflexible. (A–D) In vivo (red)– and in vitro (blue)–differentiated Th17 cells were treated for 1 h with DMSO or oligomycin (1 μ M) and then stimulated with PMA/ionomycin. OCR was analyzed on a Seahorse bioanalyzer (A); intracellular ATP was evaluated by bioluminescence (B and C); and ECAR was analyzed on a Seahorse bioanalyzer (D). (B and C) Results are expressed as percentage of DMSO-treated cells. (C) Arrows indicate time in which intracellular ATP was evaluated. (A–D) Representative of three independent experiments. Error bars represent SEM. * p < 0.001 (unpaired Student t test). n.s., not significant.



in vivo–differentiated Th17 cells (Fig. 3D). Next, we modulated the increase in glycolysis caused by oligomycin to the extent necessary to maintain lactate production at basal levels by partially blocking glycolysis (by inhibiting hexokinase 2 with 2-deoxyglucose [2-DG]) concurrent with oligomycin treatment. Lactate production increased ≥ 2 -fold when in vitro effector Th17 cells were treated with oligomycin in the absence of 2-DG, but it did not increase in the in vivo–differentiated Th17 cells (Fig. 4A). In comparison, treatment with 2-DG inhibited the oligomycin-induced increase in lactate production from in vitro effector Th17 cells (Fig. 4A) to the level observed in the in vivo effector Th17 cells. Importantly, cotreatment with 2-DG sensitizes in vitro–differentiated Th17 cells to oligomycin, causing both intracellular ATP and IL-17 to fall by $>90\%$ (Fig. 4B, 4C). From these results, we conclude that the ability to increase glycolysis to generate ATP in response to energy

restriction allows in vitro–differentiated Th17 cells to function independently of OXPHOS. This property is not observed with in vivo Th17 cells, thus rendering them exquisitely susceptible to OXPHOS inhibition.

To further confirm that Th17 cells in vivo but not those in vitro rely on OXPHOS for IL-17 production, oligomycin was applied to 1) in vivo–differentiated Th17 cells, 2) naive CD4 T cells differentiated in vitro using anti-CD3 plus anti-CD28-coated plates, and 3) OT-II splenocytes differentiated in vitro to Th17 cells by OVA Ag in the presence or absence of muramyl dipeptide, the active component of adjuvant CFA (30, 31) that was used for in vivo Th17 differentiation (Supplemental Fig. 3B, 3C, 3E). Oligomycin inhibited IL-17 production in the in vivo–differentiated Th17 cells, whereas in vitro–differentiated Th17 cells were insensitive, irrespective of the differentiation protocol used.

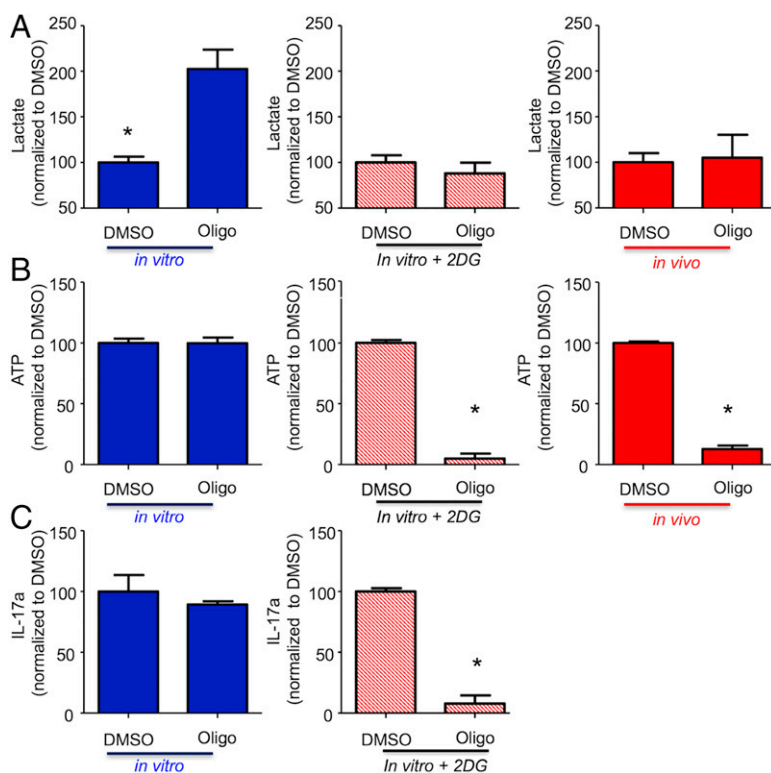


FIGURE 4. In vivo–differentiated Th17 cells have restricted glycolytic capacity. (A–C) In vivo–differentiated Th17 (red), in vitro Th17 (blue), and in vitro Th17 treated with 2-DG (red stripes) were treated for 1 h with DMSO or oligomycin (1 μ M) and then stimulated with PMA/ionomycin. Lactate concentration in cell-free supernatant from triplicate cultures was evaluated by a colorimetric assay (A), intracellular ATP triplicate cultures by bioluminescence (B), and IL-17 production in cell-free supernatant from triplicate cultures was analyzed by ELISA (C). (A–C) Results are expressed as percentage of DMSO-treated cells. (A–C) Representative of three independent experiments. Error bars represent mean \pm SEM. * p < 0.001 (unpaired Student t test).

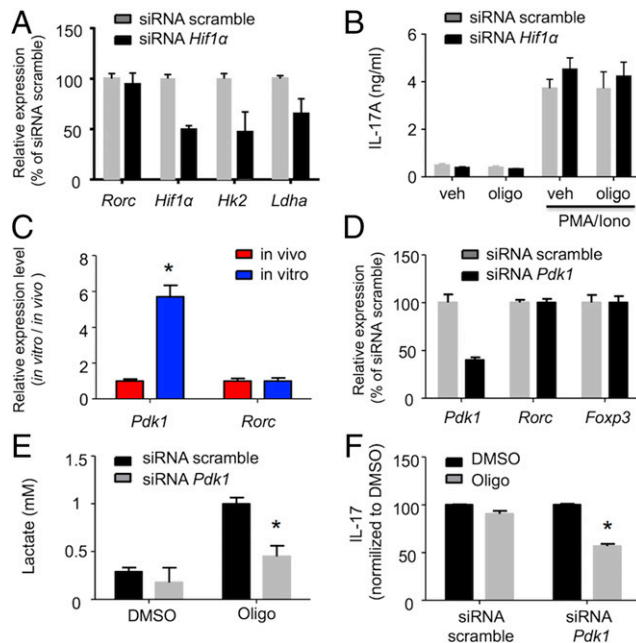


FIGURE 5. Pdk1 regulates in vitro Th17 metabolic flexibility. (A, B, and D–F) In vitro–differentiated Th17 cells were nucleofected with siRNA scramble or siRNA targeting HIF1 α (A and B) or Pdk1 (D–F) and were treated for 1 h with DMSO or oligomycin (1 μ M) and then stimulated with PMA/ionomycin. Gene expression level was analyzed by RT-PCR (A and D), lactate concentration in cell-free supernatant from triplicate cultures was determined by a colorimetric assay (E), and IL-17 production in cell-free supernatant from triplicate cultures was analyzed by ELISA (B and F). (C) Gene expression in vivo–differentiated Th17 (red) and in vitro–differentiated Th17 (blue) cells was analyzed by RT-PCR. Results are representative of two (C) and three (A, B, and D–F) independent experiments. Error bars represent mean \pm SEM. * p < 0.05 (unpaired Student t test).

Because IL-1 β and IL-2 can regulate glycolysis in T cells (32, 33), we differentiated naive CD4 cells with a polarization mixture in the presence or absence of IL-1 β , with or without IL-2 blocking Abs. Consistent with the literature (34, 35), the absence of IL-1 β reduced the number of Th17 cells from ~25 to ~5% (Supplemental Fig. 3B) whereas IL-2 blocking Abs increased the number of Th17 from ~25 to ~80% (Supplemental Fig. 3D), confirming their biological activity. Moreover, in vitro–differentiated Th17 cells were insensitive to oligomycin, irrespective of whether IL-1 β and IL-2 blocking Abs were present during the differentiation (Supplemental Fig. 3B, 3D). As Th17 differentiated in vitro with several different protocols are all insensitive to oligomycin, the reliance on OXPHOS for cytokine production appears to be a distinctive feature of in vivo–derived Th17 cells.

Glutamine metabolism is not affected by Th17 differentiation conditions

Glucose and glutamine are two of the primary carbon substrates across many aspects of T cell biology (3). These nutrients are able to displace one another in important metabolic pathways, including mitochondrial metabolism in the TCA cycle (3). Given the increased utilization of glycolysis in in vitro cells, and the increased reliance of in vivo cells on mitochondrial metabolism, we predicted that the in vivo cells would more avidly metabolize glutamine carbon in the mitochondria. To test this hypothesis, we traced glucose and glutamine carbon into intermediary metabolism using the nonradioactive carbon-13 isotope and targeted mass spectrometry–based metabolomics (24). The data from these studies confirmed the glycolytic phenotype of the in vitro Th17 cells, and surprisingly revealed that the in vitro cells were gen-

erally more metabolic—consuming and metabolizing both more glucose and more glutamine carbon (data not shown). However, when glucose and glutamine entry into the TCA cycle was analyzed as a function of total carbon, major global differences were not observed (data not shown). These results suggest that in vivo–differentiated Th17 cells do not rely on glutamine metabolism to fuel the TCA cycle, and that the major difference between in vivo and in vitro Th17 cells is at the level of glycolytic flux.

Pdk1 controls the metabolic flexibility of Th17 cells in vitro

We next sought to identify molecular differences between in vitro– and in vivo–differentiated Th17 cells to define the mechanism of metabolic flexibility. Established glycolytic activators during Th17 differentiation include HIF1 α and Pdk1. HIF1 α is transiently upregulated in normoxic conditions during Th17 cell differentiation (13, 17) (Supplemental Fig. 3F). There is evidence that HIF1 α -driven glycolysis skews differentiation of T cells toward a Th17 phenotype (13, 17); however, its role in the bioenergetics of already differentiated Th17 has not been defined. When HIF1 α in in vitro–differentiated Th17 cells was reduced by siRNA transfection, there was a slight reduction in the expression of glycolytic enzymes (Fig. 5A); however, the expression of ROR γ t remained constant and production of IL-17 was comparable to cells transfected with scramble siRNA. These data suggest that HIF1 α is important during Th17 differentiation (17, 36) but is dispensable for IL-17 production in differentiated Th17 cells (Fig. 5B). Moreover, in cells transfected with either control siRNA or with HIF1 α siRNA, treatment with oligomycin did not reduce lactate or IL-17 production (Fig. 5B, Supplemental Fig. 3G), indicating that HIF1 α expression does not control sensitivity to oligomycin and dependence on OXPHOS.

Pdk1 inhibits the pyruvate dehydrogenase complex, which leads to an increase in pyruvate to lactate conversion and a reduction of mitochondrial pyruvate oxidation. Indeed, Pdk1 expression was nearly 6-fold higher in the cells derived in vitro than in those derived in vivo (Fig. 5C). As expected, siRNA knockdown of Pdk1 expression in differentiated Th17 cells did not affect expression of either ROR γ t or Foxp3 (Fig. 5D). In contrast, lowering Pdk1 expression significantly reduced the amount of lactate produced in response to oligomycin (Fig. 5E) and made cells dependent on OXPHOS for IL-17 production (Fig. 5F). Thus, we deduce that Pdk1 provides metabolic flexibility to in vitro Th17 effectors and that low Pdk1 expression by in vivo cells can account for their OXPHOS-dependent phenotype.

Th17 cells employ OXPHOS for cytokine production in vivo

A primary function of effector Th17 cells is the secretion of cytokines such as IL-17 (37). Synthesis and secretion of cytokines are energy-intensive processes that cease when intracellular ATP is reduced (38). Hence, we sought to determine whether the metabolic differences between the in vitro– and in vivo–differentiated cells are important for this Th17 effector function by examining IL-17 expression following OXPHOS inhibition.

Treating in vivo–derived effector Th17 cells with oligomycin for 1 h ex vivo reduced IL-17 $^{+}$ cells by 40–60% (Fig. 6A), along with the amounts of IL-17 (Fig. 6B) and other Th17 signature cytokines such as GM-CSF, TNF, and IL-21 that were secreted (Fig. 6C–F). In contrast, oligomycin had a much smaller effect on IL-17 production by in vitro effector Th17 cells (10–30% decrease in CD4 $^{+}$ IL-17 $^{+}$ cells and 30–40% decrease in IL-17 titer) (Fig. 6C–F). The differential sensitivity of IL-17 production to oligomycin is independent of when oligomycin is added relative to the time at which cells are analyzed and the specific polarization mixture employed (Supplemental Fig. 3). Taken together, these results show that in vivo–differentiated Th17 cells rely on

OXPHOS for cytokine production and suggest that Th17 function *in vivo* can be modulated by inhibition of oxidative metabolism.

Modulating OXPHOS regulates Th17 effector function *in vivo*

We sought to determine whether the metabolic sensitivity of IL-17 production to oligomycin identified *ex vivo* is also observed *in vivo*. For these experiments, mice were injected with anti-CD3 Ab to induce IL-17 production in the presence or absence of oligomycin, and plasma levels of IL-17 were measured. To confirm that the IL-17 produced in this model is ROR γ t-dependent, a control group of animals received ursolic acid (an ROR γ t inhibitor) together with the anti-CD3 Ab (39). Both oligomycin and ursolic acid reduced IL-17 serum to similar levels (Fig. 7A). Notably, this effect was specific for Th17 cells, as production of other cytokines (e.g., TNF; Fig. 7B) was not affected. In contrast, echinomycin, which was effective in blocking the transcription of HIF1 α target genes *in vivo* (Fig. 7C), had no effect on anti-CD3-induced IL-17, indicating that HIF1 α does not regulate Th17 effector function *in vivo* (Fig. 7A, right).

To test whether inhibiting OXPHOS controls inflammatory cytokine production *in vivo*, we assessed the effect of oligomycin in a murine TNBS colitis model in which development of disease is IL-17-dependent (40). In this model, oligomycin was comparable to ursolic acid in reducing disease (Fig. 7D, 7E). To further evaluate the role of OXPHOS in IL-17 production *in vivo*, we next tested the effect of oligomycin and ursolic acid in a murine IL-17-driven model of psoriasis (41, 42). In this model, oligomycin reduced ear thickness, keratinocyte proliferation, and immune cell infiltration (Fig. 7F, 7G). The efficacy of oligomycin in this model was comparable to ursolic acid.

To determine whether oligomycin reduces IL-17 production directly on cells isolated from sites of inflammation, LPMCs were isolated from mice with colitis and healthy controls and treated *ex vivo* with oligomycin before stimulation with PMA and ionomycin. Because the CD4 Ag is cleaved during isolation of LPMCs, we compared the effect of oligomycin on total CD3⁺ cells relative to CD3⁺CD8⁺ cells. Animals with colitis had almost 3-fold more CD3⁺IL-17⁺IFN- γ ⁺ cells relative to controls (Fig. 8A, Supplemental Fig. 4A, 4B, 4E), and oligomycin reduced the number of CD3⁺IL-17⁺IFN- γ ⁺ cells in LPMCs from mice with colitis by ~70% (Fig. 8B, Supplemental Fig. 4B, 4E). In contrast, oligomycin had no effect on the production of IL-17 in CD3⁺CD8⁺ cells, and only slightly increased the number of CD3⁺CD8⁺IFN- γ ⁺ cells (Fig. 8C), consistent with the glycolytic phenotype of CD8⁺ effector cells (Fig. 2A). From these results we conclude that, similar to the bioenergetic requirements of effector Th17 cells generated by adjuvant challenge *in vivo*, OXPHOS is required for IL-17 production by Th17 cells at sites of colonic inflammation.

We next asked whether OXPHOS supports the IL-17 production by differentiated human Th17 cells. To address this question, purified PBMCs from healthy subjects and patients with IBD were stimulated with PMA and ionomycin. Oligomycin reduced IL-17 expression and secretion in CD4⁺ lymphocytes from both healthy subjects and patients with IBD, whereas echinomycin, an inhibitor of HIF1 α , had no effect (data not shown). Other Th17 cytokines, including TNF and GM-CSF, were also sensitive to oligomycin and unaffected by echinomycin (data not shown). Thus, the secretion of cytokines by human Th17 cells isolated from blood depends on OXPHOS, similar to murine Th17 effector cells generated *in vivo*.

Lastly, LPMCs were purified from human tissue biopsied at sites of inflammation identified by endoscopy in subjects with active IBD. After isolation, cells were stimulated with PMA and ionomycin in the absence or presence of oligomycin. Oligomycin significantly decreased the percentage of CD3⁺IL-17⁺IFN- γ ⁺ and T cells, producing both IFN- γ and IL-17, whereas the proportion of CD3⁺IFN- γ ⁺IL-17⁺ was not changed (Fig. 8D). These data provide evidence that human Th17 cells at sites of colonic inflammation selectively depend on OXPHOS for their function, similar to murine Th17 cells generated *in vivo*, thereby rendering them susceptible to OXPHOS inhibitors. These results also underscore the importance of using *in vivo* models to understand metabolic control of T cell function (43).

Discussion

In this study, we show that the environment in which naive T lymphocytes differentiate into effector Th17 cells has a profound influence on their metabolism after differentiation. Th17 cells differentiated *in vitro* are metabolically flexible and meet the bioenergetic demands of cytokine production (which can account for up to 50% of total cellular ATP requirements in lymphocytes) (38) using either OXPHOS or glycolysis (Fig. 8E). These results are consistent with previous studies showing that lymphocytes are metabolically flexible *in vitro* and can upregulate glycolysis when OXPHOS is inhibited or when certain nutrients are limiting (44), a feature thought to promote lymphocyte fitness (45). In contrast, Th17 cells derived *in vivo* rely on OXPHOS to supply ATP needed for cytokine production (Fig. 8E). The finding that *in vivo*-derived effector Th17 cells are metabolically inflexible and cannot upregulate glycolysis when bioenergetically challenged was unexpected. This result has significant implications for the discovery and development of therapeutics to control immune responses, in that the inability to compensate to metabolic stress renders Th17 cells vulnerable to drugs that target their metabolism (4).

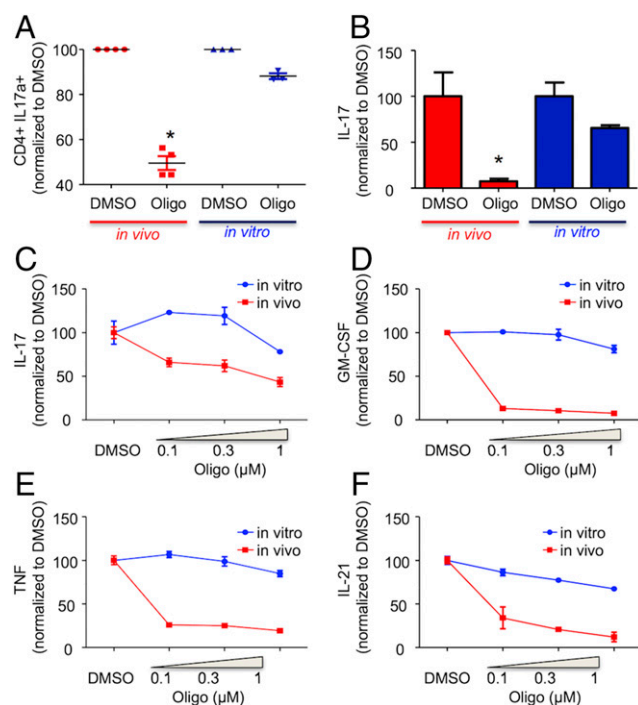


FIGURE 6. OXPHOS inhibition reduces Th17 cytokine production. (A–F) *In vivo* (red)– or *in vitro* (blue)–differentiated Th17 cells were treated for 1 h with DMSO or the indicated concentration of oligomycin and then stimulated with PMA/ionomycin. IL-17 expression was analyzed by FACS (A). The production of IL-17a, GM-CSF, TNF, and IL-21 in cell-free supernatant from triplicate cultures was evaluated by ELISA (B–F). (A–F) Results are expressed as percentage of DMSO-treated cells. (A) For *in vivo* Th17, each dot represents an individual mouse; for *in vitro* Th17, an independent cell culture. (A–F) Representative of three independent experiments. Error bars represent mean ± SEM. **p* < 0.001 [(A) paired Student *t* test; (B–F) unpaired Student *t* test].

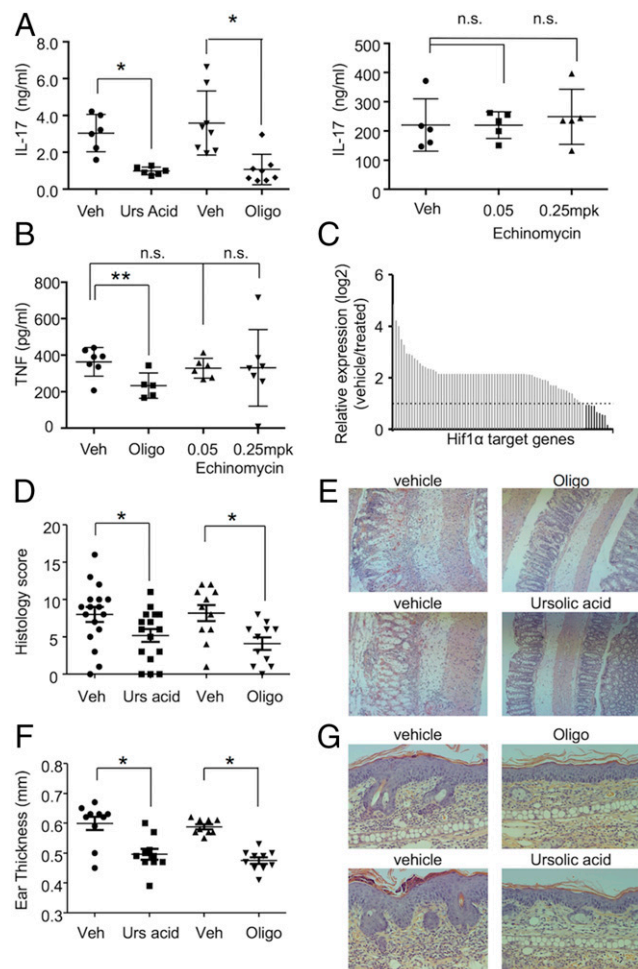


FIGURE 7. OXPHOS inhibition reduces IL-17 production in vivo. (**A–C**) Mice were treated via i.p. injection with vehicle, ursolic acid (**A**), oligomycin (**A** and **B**), and echinomycin for 1 h and then stimulated i.p. with agonistic anti-CD3ε Ab for 3 h. (**A** and **B**) IL-17a (**A**) and TNF (**B**) plasma concentrations were determined by ELISA. (**C**) Expression of HIF1α target genes was analyzed using RNA extracted from at least three spleens per treatment group by quantitative PCR and expressed as a ratio between vehicle and 0.25 mg/kg echinomycin-treated animals. Dashed line depicts the cutoff of >2-fold difference. Dark gray bars show higher expression in vehicle-treated samples. (**D** and **E**) B6 mice were dosed with oligomycin or ursolic acid and then challenged intrarectally with TNBS. (**D**) Graph shows histology score of individual mice 2 d after TNBS challenge. (**E**) Representative images. (**F** and **G**) B6 mice dosed with oligomycin or ursolic acid followed by daily application of Aldara cream. (**F**) Graph shows ear thickness of individual mice 5 d after Aldara treatment. (**G**) Representative histology. (**E** and **G**) H&E, original magnification $\times 40$. (**A**, **B**, **D**, and **F**) Each dot represents an individual mouse. (**A**, **C**, and **F**) Representative of three independent experiments. (**D**) Results from two independent experiments are plotted together. Error bars represent mean \pm SEM. * $p < 0.001$, ** $p < 0.05$ (unpaired Student *t* test). n.s., not significant.

The dependence of effector Th17 cells on oxidative metabolism in vivo contrasts with the glycolytic phenotype described for other proinflammatory lineages of differentiated CD4 cells (14, 26) and for CD8 effector cells (46, 47) and is comparable to the metabolic phenotype of memory CD8 cells that require OXPHOS for survival and function (48, 49). Both memory CD8 T cells and Th17 cells can survive in vivo for extended periods and produce more differentiated progeny (50, 51); hence, it is possible that dependence of Th17 cells on OXPHOS is linked to this enhanced survival advantage in vivo. In support of this hypothesis, increased

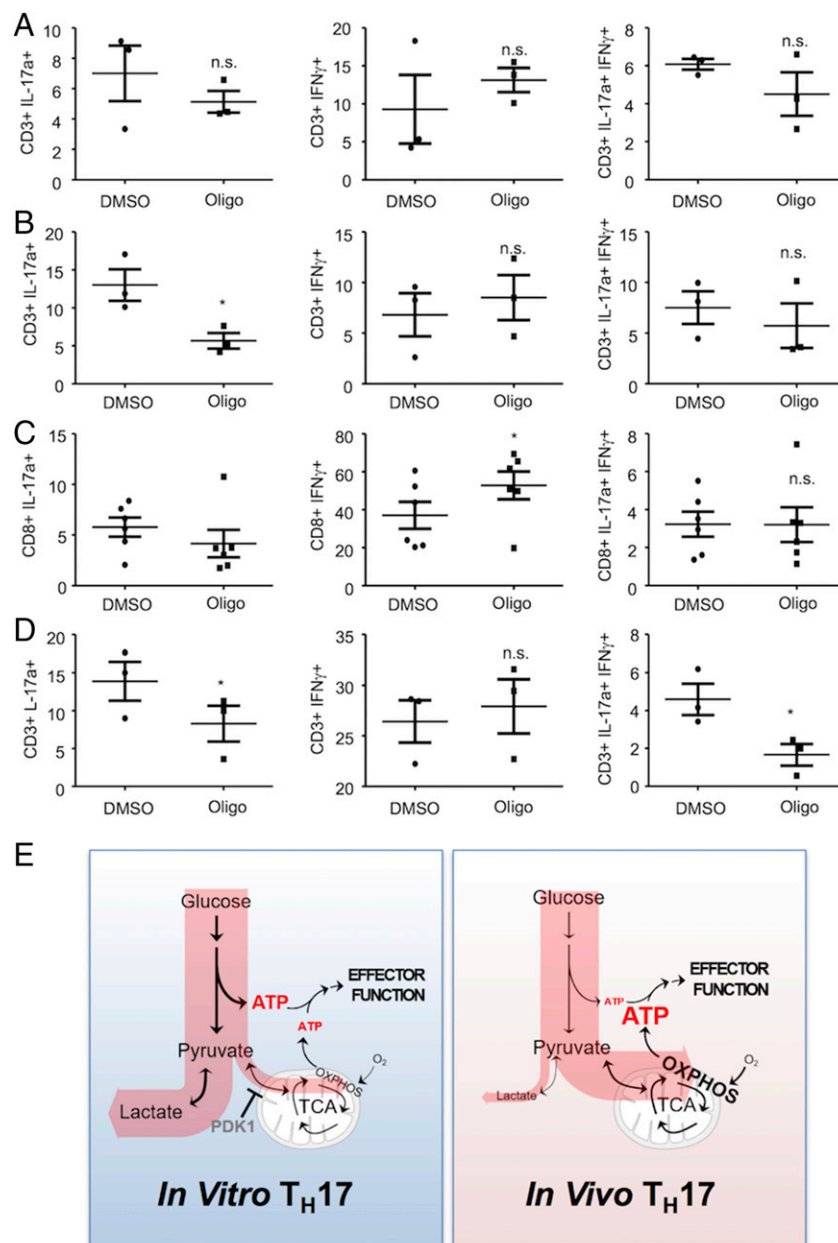
oxidative metabolism promotes stemness and survival in CD8 cells (43, 52). Similarly, Kawalekar et al. (53) showed that 4-1BBζ CAR T cells are characterized by increased central memory differentiation, along with enhanced mitochondrial biogenesis, and greater oxidative metabolism compared with Ag-stimulated CD28ζ CAR T cells. These data further support the hypothesis that increased oxidative phosphorylation with limited glycolysis is necessary for central memory differentiation and long-term survival (43, 54).

A key outstanding question regarding the metabolism of immune cells is how environmental cues influence the metabolic pathways that shape immune responses (3, 20). Environmental signals in vitro, in the form of nutrient availability, oxygen tension, cytokine concentration, and length and type of cellular stimulation, are all known to affect cellular bioenergetics (reviewed in Ref. 3). To probe the possibility that the metabolism of effector Th17 cells varies as a result of the context in which they are found, we assessed the bioenergetics of Th17 cells isolated from different anatomical loci and at sites of inflammation, which differ with respect to nutrient availability and cytokine levels (20). This point is quite relevant in the intestine, where the microenvironment contains substrates derived from food, as well as unique metabolites from the intestinal microbiome that can impact immune responses and that are not present in lymph nodes (55). Notwithstanding, we found that Th17 cells isolated from the lymph nodes, spleen, and thymus (data not shown) of immunized mice, human peripheral blood, and cells isolated from inflamed lamina propria all employ OXPHOS to generate the energy required for production of IL-17. These data indicate that the bioenergetics of Th17 cells are independent of the specific compartment from which cells are isolated and suggest that the observed oxidative phenotype is an intrinsic property of in vivo-differentiated Th17 cells. Given that limited oxygen availability in the inflamed intestine can promote glycolysis (20), the finding that Th17 derived from oxygen-poor sites of inflammation retain an oxidative phenotype suggests that the environment in which Th17 cells differentiate instructs their metabolic fate, as opposed to the environments in which they function. However, we cannot exclude the possibility that Th17 effector cells isolated from other tissues and microenvironments, such as tumors, have alternate metabolic programs that more closely match that of in vitro-derived Th17 cells (20). Collectively, our data are consistent with other studies showing that immune cells adapt specific metabolic phenotypes in vivo (21, 22, 56); hence, conclusions about metabolism and energy production by immune cells should not be based entirely on results from in vitro models.

We explored the basis for the difference in metabolic flexibility between in vitro and in vivo Th17 cells. HIF1α is activated by reduced O₂ tension and in normoxic conditions by inflammatory cytokines, reactive oxygen species, growth factors, and bacterial products (57). Even though HIF1α is necessary for Th17 cell differentiation (13, 17) and promotes glycolysis in immune cells (20), reducing its expression in differentiated Th17 cells had no effect on IL-17 production, even when mitochondrial ATP production was inhibited. These findings suggest that differences in the metabolic programs of in vitro and in vivo Th17 cells do not result from differential expression of HIF1α and are consistent with transient expression of HIF1α during Th17 cell differentiation (Supplemental Fig. 3F) (17, 36).

Pdk1 is another gene that regulates glucose metabolism. By inhibiting the activity of the pyruvate dehydrogenase complex, Pdk1 increases the rate that glucose-derived pyruvate is converted into lactate (58). The expression of Pdk1 is regulated by nutrient levels and several signaling pathways (59, 60), and it is expressed

FIGURE 8. OXPHOS controls IL-17 production in IBD. (A–D) LPMCs that were isolated from mice treated with ethanol (A) or TNBS (B and C), or from human IBD patients (D), were treated for 1 h with DMSO or oligomycin (1 μ M) and then stimulated with PMA/ionomycin. IL-17 and IFN- γ production in CD3⁺ and CD8⁺ was evaluated by FACS analysis. Each dot represents an individual mouse (A–C) or subject (D). (A–C) Representative of three independent experiments. Error bars represent mean \pm SEM. (E) Schematic representation of the metabolic pathways used to fuel effector function in Th17 cells. Th17 cells derived in vitro predominantly use glycolysis to generate ATP to sustain effector function (left). Additionally, these cells exhibit metabolic flexibility and can engage OXPHOS-derived ATP when glycolysis is inhibited. Th17 cells derived in vivo (right) generate ATP used to sustain effector function through mitochondrial OXPHOS and are unable to engage glycolysis to sustain ATP levels following OXPHOS inhibition. * $p < 0.05$ (paired Student t test). n.s., not significant.



in in vitro-differentiated Th17 cells at a >6-fold excess of in vivo-differentiated cells. Gerriets et al. recently found that by increasing glycolysis, Pdk1 drives Th17 differentiation in vitro (16). In addition to functioning during Th17 differentiation, our data show that Pdk1 activity has a role in IL-17 production in in vitro-differentiated Th17 cells under metabolic stress, but that Pdk1 does not affect in vivo-derived Th17 cell metabolism. Furthermore, low Pdk1 expression in Th17 cells generated in vivo likely explains their particular dependence on OXPHOS for IL-17 production.

The Crabtree effect is a phenomenon whereby exposure to a high concentration of glucose limits OXPHOS (61). Unlike with the Warburg effect, cells retain the ability to switch to mitochondrial respiration when glycolysis is inhibited (61). The Crabtree effect has been observed in lymphocytes (62) and cancer cells (61), but the underlying molecular mechanism remains poorly characterized. In vitro, Th17 cells are exposed to a high concentration of glucose (≥ 11 mM versus 4 mM in vivo), and glucose concentration can drive the expression of Pdk1 (60). An intriguing pos-

sibility is that the metabolic phenotype of in vitro Th17 cells can be explained by the Crabtree effect and that the Crabtree effect is regulated at a molecular level by the expression of Pdk1. Additional studies are required to test this hypothesis.

Th17 cells are a central component of immune host defense. There is evidence that these cells also contribute to pathological inflammation associated with autoimmune diseases, including IBD (6, 63) and psoriasis (41, 42). The critical role of IL-17 in psoriasis is documented by the efficacy of anti-IL-17A Abs (64), but blocking IL-17A alone is not sufficient to limit colitis (65), suggesting that therapeutic interventions in IBD need to target a more complete spectrum of Th17 effector functions. In agreement with this hypothesis, adoptive transfer experiments have shown that Th17 cells are more effective than Th1 in inducing murine colitis (65), Th17 cells accumulate in intestinal inflammatory lesions in IBD (66, 67), and that genetic polymorphism of cytokines controlling Th17 generation and function is associated with an increased risk of IBD (68). The metabolic dependence of in vivo-derived Th17 cells on OXPHOS provides the possibility of controlling Th17 cell-driven

disease by restricting OXPHOS. In this study, we showed that oligomycin, a specific and potent inhibitor of OXPHOS, reduced key Th17 cytokines produced by human and murine cells, is effective in blocking Th17 effector functions in cells from sites of colonic inflammation, and controls disease in murine TNBS-induced colitis and psoriasis. The differences in the metabolic pathways available to Th17 effector cells generated in vitro and in vivo highlight the importance of studying metabolism in vivo, particularly with respect to designing interventions that exploit cellular bioenergetics and support the concept that modulation of OXPHOS has therapeutic potential for diseases driven by Th17 cells.

Acknowledgments

We thank Andrea Viale (MD Anderson Cancer Center) for experimental advice.

Disclosures

L.F., L.-Y.H., M.A.S., X.L., K.D., C.A.L., B.S., X.H., A.W.O., and G.D.G. have ownership interests in Lycera Corporation. The other authors have no financial conflicts of interest.

References

- Pearce, E. L., and E. J. Pearce. 2013. Metabolic pathways in immune cell activation and quiescence. *Immunity* 38: 633–643.
- MacIver, N. J., R. D. Michalek, and J. C. Rathmell. 2013. Metabolic regulation of T lymphocytes. *Annu. Rev. Immunol.* 31: 259–283.
- Wahl, D. R., C. A. Byersdorfer, J. L. Ferrara, A. W. Opipari, Jr., and G. D. Glick. 2012. Distinct metabolic programs in activated T cells: opportunities for selective immunomodulation. *Immunol. Rev.* 249: 104–115.
- O'Sullivan, D., and E. L. Pearce. 2015. Targeting T cell metabolism for therapy. *Trends Immunol.* 36: 71–80.
- Peters, A., Y. Lee, and V. K. Kuchroo. 2011. The many faces of Th17 cells. *Curr. Opin. Immunol.* 23: 702–706.
- Huber, S., N. Gagliani, and R. A. Flavell. 2012. Life, death, and miracles: Th17 cells in the intestine. *Eur. J. Immunol.* 42: 2238–2245.
- O'Connor Jr., W., L. A. Zelenewicz, and R. A. Flavell. 2010. The dual nature of Th17 cells: shifting the focus to function. *Nat. Immunol.* 11: 471–476.
- Lee, Y., A. Awasthi, N. Yosef, F. J. Quintana, S. Xiao, A. Peters, C. Wu, M. Kleinewietfeld, S. Kunder, D. A. Hafler, et al. 2012. Induction and molecular signature of pathogenic Th17 cells. *Nat. Immunol.* 13: 991–999.
- Zielinski, C. E., F. Mele, D. Aschenbrenner, D. Jarrossay, F. Ronchi, M. Gattorno, S. Monticelli, A. Lanzavecchia, and F. Sallusto. 2012. Pathogen-induced human Th17 cells produce IFN- γ or IL-10 and are regulated by IL-1 β . *Nature* 484: 514–518.
- Hu, X., Y. Wang, L. Y. Hao, X. Liu, C. A. Lesch, B. M. Sanchez, J. M. Wendling, R. W. Morgan, T. D. Aicher, L. L. Carter, et al. 2015. Corrigendum: sterol metabolism controls Th17 differentiation by generating endogenous ROR γ agonists. *Nat. Chem. Biol.* 11: 741.
- Semenza, G. L. 2011. Regulation of metabolism by hypoxia-inducible factor 1. *Cold Spring Harb. Symp. Quant. Biol.* 76: 347–353.
- Saunier, E., C. Benelli, and S. Bortoli. 2016. The pyruvate dehydrogenase complex in cancer: an old metabolic gatekeeper regulated by new pathways and pharmacological agents. *Int. J. Cancer* 138: 809–817.
- Shi, L. Z., R. Wang, G. Huang, P. Vogel, G. Neale, D. R. Green, and H. Chi. 2011. HIF1 α -dependent glycolytic pathway orchestrates a metabolic checkpoint for the differentiation of Th17 and T_{reg} cells. *J. Exp. Med.* 208: 1367–1376.
- Michalek, R. D., V. A. Gerriets, S. R. Jacobs, A. N. Macintyre, N. J. MacIver, E. F. Mason, S. A. Sullivan, A. G. Nichols, and J. C. Rathmell. 2011. Cutting edge: distinct glycolytic and lipid oxidative metabolic programs are essential for effector and regulatory CD4⁺ T cell subsets. *J. Immunol.* 186: 3299–3303.
- Delgoffe, G. M., K. N. Pollizzi, A. T. Waickman, E. Heikamp, D. J. Meyers, M. R. Horton, B. Xiao, P. F. Worley, and J. D. Powell. 2011. The kinase mTOR regulates the differentiation of helper T cells through the selective activation of signaling by mTORC1 and mTORC2. *Nat. Immunol.* 12: 295–303.
- Gerriets, V. A., R. J. Kishton, A. G. Nichols, A. N. Macintyre, M. Inoue, O. Ilkayeva, P. S. Winter, X. Liu, B. Priyadharshini, M. E. Slawinska, et al. 2015. Metabolic programming and PDHK1 control CD4⁺ T cell subsets and inflammation. *J. Clin. Invest.* 125: 194–207.
- Dang, E. V., J. Barbi, H. Y. Yang, D. Jinasena, H. Yu, Y. Zheng, Z. Bordin, J. Fu, Y. Kim, H. R. Yen, et al. 2011. Control of Th17/T_{reg} balance by hypoxia-inducible factor 1. *Cell* 146: 772–784.
- Berod, L., C. Friedrich, A. Nandan, J. Freitag, S. Hagemann, K. Harmrolfs, A. Sandouk, C. Hesse, C. N. Castro, H. Bähre, et al. 2014. De novo fatty acid synthesis controls the fate between regulatory T and T helper 17 cells. *Nat. Med.* 20: 1327–1333.
- Pollizzi, K. N., and J. D. Powell. 2014. Integrating canonical and metabolic signalling programmes in the regulation of T cell responses. *Nat. Rev. Immunol.* 14: 435–446.
- Pearce, E. L., M. C. Poffenberger, C. H. Chang, and R. G. Jones. 2013. Fueling immunity: insights into metabolism and lymphocyte function. *Science* 342: 1242–1245.
- Gatza, E., D. R. Wahl, A. W. Opipari, T. B. Sundberg, P. Reddy, C. Liu, G. D. Glick, and J. L. Ferrara. 2011. Manipulating the bioenergetics of alloreactive T cells causes their selective apoptosis and arrests graft-versus-host disease. *Sci. Transl. Med.* 3: 67ra8.
- Procaccini, C., F. Carbone, D. Di Silvestre, F. Brambilla, V. De Rosa, M. Galgani, D. Faicchia, G. Marone, D. Tramontano, M. Corona, et al. 2016. The proteomic landscape of human ex vivo regulatory and conventional T cells reveals specific metabolic requirements. [Published erratum appears in 2016 *Immunity* 44: 712.] *Immunity* 44: 406–421.
- Monteleone, G., L. Biancone, R. Marasco, G. Morrone, O. Marasco, F. Luzzo, and F. Pallone. 1997. Interleukin 12 is expressed and actively released by Crohn's disease intestinal lamina propria mononuclear cells. *Gastroenterology* 112: 1169–1178.
- Son, J., C. A. Lyssiotis, H. Ying, X. Wang, S. Hua, M. Ligorio, R. M. Perera, C. R. Ferrone, E. Mullarky, N. Shyh-Chang, et al. 2013. Glutamine supports pancreatic cancer growth through a KRAS-regulated metabolic pathway. *Nature* 496: 101–105.
- Yuan, M., S. B. Breitkopf, X. Yang, and J. M. Asara. 2012. A positive/negative ion-switching, targeted mass spectrometry-based metabolomics platform for bodily fluids, cells, and fresh and fixed tissue. *Nat. Protoc.* 7: 872–881.
- Chang, C. H., J. D. Curtis, L. B. Maggi, Jr., B. Faubert, A. V. Villarino, D. O'Sullivan, S. C. Huang, G. J. van der Windt, J. Blagih, J. Qiu, et al. 2013. Posttranscriptional control of T cell effector function by aerobic glycolysis. *Cell* 153: 1239–1251.
- Glick, G. D., R. Rossignol, C. A. Lyssiotis, D. Wahl, C. Lesch, B. Sanchez, X. Liu, L. Y. Hao, C. Taylor, A. Hurd, et al. 2014. Anaplerotic metabolism of alloreactive T cells provides a metabolic approach to treat graft-versus-host disease. *J. Pharmacol. Exp. Ther.* 351: 298–307.
- Berridge, M. V., P. M. Herst, and A. S. Tan. 2010. Metabolic flexibility and cell hierarchy in metastatic cancer. *Mitochondrion* 10: 584–588.
- Viale, A., P. Pettazzoni, C. A. Lyssiotis, H. Ying, N. Sánchez, M. Marchesini, A. Carugo, T. Green, S. Seth, V. Giuliani, et al. 2014. Oncogene ablation-resistant pancreatic cancer cells depend on mitochondrial function. *Nature* 514: 628–632.
- Ellouz, F., A. Adam, R. Ciorbaru, and E. Lederer. 1974. Minimal structural requirements for adjuvant activity of bacterial peptidoglycan derivatives. *Biochem. Biophys. Res. Commun.* 59: 1317–1325.
- Adam, A., R. Ciorbaru, F. Ellouz, J. F. Petit, and E. Lederer. 1974. Adjuvant activity of monomeric bacterial cell wall peptidoglycans. *Biochem. Biophys. Res. Commun.* 56: 561–567.
- Chatterjee, S., K. Thyagarajan, P. Kesarwani, J. H. Song, M. Soloshchenko, J. Fu, S. R. Bailey, C. Vasu, A. S. Kraft, C. M. Paulos, et al. 2014. Reducing CD73 expression by IL1 β -programmed Th17 cells improves immunotherapeutic control of tumors. *Cancer Res.* 74: 6048–6059.
- Ray, J. P., M. M. Staron, J. A. Shyer, P. C. Ho, H. D. Marshall, S. M. Gray, B. J. Laidlaw, K. Araki, R. Ahmed, S. M. Kaech, and J. Craft. 2015. The interleukin-2-mTORC1 kinase axis defines the signaling, differentiation, and metabolism of T helper 1 and follicular B helper T cells. *Immunity* 43: 690–702.
- Chung, Y., S. H. Chang, G. J. Martinez, X. O. Yang, R. Nurieva, H. S. Kang, L. Ma, S. S. Watowich, A. M. Jetten, Q. Tian, and C. Dong. 2009. Critical regulation of early Th17 cell differentiation by interleukin-1 signaling. *Immunity* 30: 576–587.
- Laurence, A., C. M. Tato, T. S. Davidson, Y. Kanno, Z. Chen, Z. Yao, R. B. Blank, F. Meylan, R. Siegel, L. Hennighausen, et al. 2007. Interleukin-2 signaling via STAT5 constrains T helper 17 cell generation. *Immunity* 26: 371–381.
- Wang, H., H. Flach, M. Onizawa, L. Wei, M. T. McManus, and A. Weiss. 2014. Negative regulation of Hif1 α expression and Th17 differentiation by the hypoxia-regulated microRNA miR-210. *Nat. Immunol.* 15: 393–401.
- Zúñiga, L. A., R. Jain, C. Haines, and D. J. Cua. 2013. Th17 cell development: from the cradle to the grave. *Immunol. Rev.* 252: 78–88.
- Krauss, S., M. D. Brand, and F. Buttgeriet. 2001. Signaling takes a breath—new quantitative perspectives on bioenergetics and signal transduction. *Immunity* 15: 497–502.
- Xu, T., X. Wang, B. Zhong, R. I. Nurieva, S. Ding, and C. Dong. 2011. Ursolic acid suppresses interleukin-17 (IL-17) production by selectively antagonizing the function of ROR γ t protein. *J. Biol. Chem.* 286: 22707–22710.
- Jin, Y., Y. Lin, L. Lin, and C. Zheng. 2012. IL-17/IFN- γ interactions regulate intestinal inflammation in TNBS-induced acute colitis. *J. Interferon Cytokine Res.* 32: 548–556.
- Cai, Y., X. Shen, C. Ding, C. Qi, K. Li, X. Li, V. R. Jala, H. G. Zhang, T. Wang, J. Zheng, and J. Yan. 2011. Pivotal role of dermal IL-17-producing $\gamma\delta$ T cells in skin inflammation. *Immunity* 35: 596–610.
- Pantelyushin, S., S. Haak, B. Ingold, P. Kulig, F. L. Heppner, A. A. Navarini, and B. Becher. 2012. Ror γ t⁺ innate lymphocytes and $\gamma\delta$ T cells initiate psoriasisiform plaque formation in mice. *J. Clin. Invest.* 122: 2252–2256.
- Chang, J. T., E. J. Wherry, and A. W. Goldrath. 2014. Molecular regulation of effector and memory T cell differentiation. *Nat. Immunol.* 15: 1104–1115.
- Tripmacher, R., T. Gaber, R. Dziurla, T. Häupl, K. Ereku, A. Grützkau, M. Tschirschmann, A. Scheffold, A. Radbruch, G. R. Burmester, and F. Buttgeriet. 2008. Human CD4⁺ T cells maintain specific functions even under conditions of extremely restricted ATP production. *Eur. J. Immunol.* 38: 1631–1642.
- Siska, P. J., and J. C. Rathmell. 2015. T cell metabolic fitness in antitumor immunity. *Trends Immunol.* 36: 257–264.

46. Doedens, A. L., A. T. Phan, M. H. Stradner, J. K. Fujimoto, J. V. Nguyen, E. Yang, R. S. Johnson, and A. W. Goldrath. 2013. Hypoxia-inducible factors enhance the effector responses of CD8⁺ T cells to persistent antigen. *Nat. Immunol.* 14: 1173–1182.
47. Gubser, P. M., G. R. Bantug, L. Razik, M. Fischer, S. Dimeloe, G. Hoenger, B. Durovic, A. Jauch, and C. Hess. 2013. Rapid effector function of memory CD8⁺ T cells requires an immediate-early glycolytic switch. *Nat. Immunol.* 14: 1064–1072.
48. Araki, K., A. P. Turner, V. O. Shaffer, S. Gangappa, S. A. Keller, M. F. Bachmann, C. P. Larsen, and R. Ahmed. 2009. mTOR regulates memory CD8 T-cell differentiation. *Nature* 460: 108–112.
49. Pearce, E. L., M. C. Walsh, P. J. Cejas, G. M. Harms, H. Shen, L. S. Wang, R. G. Jones, and Y. Choi. 2009. Enhancing CD8 T-cell memory by modulating fatty acid metabolism. *Nature* 460: 103–107.
50. Kryczek, L., E. Zhao, Y. Liu, Y. Wang, L. Vatan, W. Szeliga, J. Moyer, A. Klimczak, A. Lange, and W. Zou. 2011. Human TH17 cells are long-lived effector memory cells. *Sci. Transl. Med.* 3: 104ra100.
51. Muranski, P., Z. A. Borman, S. P. Kerkar, C. A. Klebanoff, Y. Ji, L. Sanchez-Perez, M. Sukumar, R. N. Reger, Z. Yu, S. J. Kern, et al. 2011. Th17 cells are long lived and retain a stem cell-like molecular signature. *Immunity* 35: 972–985.
52. Sukumar, M., J. Liu, Y. Ji, M. Subramanian, J. G. Crompton, Z. Yu, R. Roychoudhuri, D. C. Palmer, P. Muranski, E. D. Karoly, et al. 2013. Inhibiting glycolytic metabolism enhances CD8⁺ T cell memory and antitumor function. *J. Clin. Invest.* 123: 4479–4488.
53. Kawalekar, O. U., R. S. O'Connor, J. A. Fraietta, L. Guo, S. E. McGettigan, A. D. Posey, Jr., P. R. Patel, S. Guedan, J. Scholler, B. Keith, et al. 2016. Distinct signaling of coreceptors regulates specific metabolism pathways and impacts memory development in CAR T cells. [Published erratum appears in 2016 *Immunity* 44: 712.] *Immunity* 44: 380–390.
54. Gattinoni, L., C. A. Klebanoff, and N. P. Restifo. 2012. Paths to stemness: building the ultimate antitumor T cell. *Nat. Rev. Cancer* 12: 671–684.
55. Sharon, G., N. Garg, J. Debelius, R. Knight, P. C. Dorrestein, and S. K. Mazmanian. 2014. Specialized metabolites from the microbiome in health and disease. *Cell Metab.* 20: 719–730.
56. De Rosa, V., M. Galgani, A. Porcellini, A. Colamatteo, M. Santopaolo, C. Zuchegna, A. Romano, S. De Simone, C. Procaccini, C. La Rocca, et al. 2015. Glycolysis controls the induction of human regulatory T cells by modulating the expression of FOXP3 exon 2 splicing variants. *Nat. Immunol.* 16: 1174–1184.
57. Semenza, G. L. 2013. HIF-1 mediates metabolic responses to intratumoral hypoxia and oncogenic mutations. *J. Clin. Invest.* 123: 3664–3671.
58. Patel, M. S., N. S. Nemeria, W. Furey, and F. Jordan. 2014. The pyruvate dehydrogenase complexes: structure-based function and regulation. *J. Biol. Chem.* 289: 16615–16623.
59. Kaplon, J., L. Zheng, K. Meissl, B. Chaneton, V. A. Selivanov, G. Mackay, S. H. van der Burg, E. M. Verdegaal, M. Cascante, T. Shlomi, et al. 2013. A key role for mitochondrial gatekeeper pyruvate dehydrogenase in oncogene-induced senescence. *Nature* 498: 109–112.
60. Xu, J., J. Han, P. N. Epstein, and Y. Q. Liu. 2006. Regulation of PDK mRNA by high fatty acid and glucose in pancreatic islets. *Biochem. Biophys. Res. Commun.* 344: 827–833.
61. Diaz-Ruiz, R., M. Rigoulet, and A. Devin. 2011. The Warburg and Crabtree effects: on the origin of cancer cell energy metabolism and of yeast glucose repression. *Biochim. Biophys. Acta* 1807: 568–576.
62. Guppy, M., E. Greiner, and K. Brand. 1993. The role of the Crabtree effect and an endogenous fuel in the energy metabolism of resting and proliferating thymocytes. *Eur. J. Biochem.* 212: 95–99.
63. Monteleone, I., M. Sarra, F. Pallone, and G. Monteleone. 2012. Th17-related cytokines in inflammatory bowel diseases: friends or foes? *Curr. Mol. Med.* 12: 592–597.
64. Mease, P. J., I. B. McInnes, B. Kirkham, A. Kavanaugh, P. Rahman, D. van der Heijde, R. Landewé, P. Nash, L. Pricop, J. Yuan, et al; FUTURE 1 Study Group. 2015. Secukinumab inhibition of interleukin-17A in patients with psoriatic arthritis. *N. Engl. J. Med.* 373: 1329–1339.
65. Leppkes, M., C. Becker, I. I. Ivanov, S. Hirth, S. Wirtz, C. Neufert, S. Pouly, A. J. Murphy, D. M. Valenzuela, G. D. Yancopoulos, et al. 2009. ROR γ -expressing Th17 cells induce murine chronic intestinal inflammation via redundant effects of IL-17A and IL-17F. *Gastroenterology* 136: 257–267.
66. Fujino, S., A. Andoh, S. Bamba, A. Ogawa, K. Hata, Y. Araki, T. Bamba, and Y. Fujiyama. 2003. Increased expression of interleukin 17 in inflammatory bowel disease. *Gut* 52: 65–70.
67. Rovedatti, L., T. Kudo, P. Biancheri, M. Sarra, C. H. Knowles, D. S. Rampton, G. R. Corazza, G. Monteleone, A. Di Sabatino, and T. T. MacDonald. 2009. Differential regulation of interleukin 17 and interferon γ production in inflammatory bowel disease. *Gut* 58: 1629–1636.
68. Graham, D. B., and R. J. Xavier. 2013. From genetics of inflammatory bowel disease towards mechanistic insights. *Trends Immunol.* 34: 371–378.